Photoelectron Spectra of Carbonyls. Oxamide, Parabanic Acid, and Their *N*-Methyl Derivatives

J. L. Meeks and S. P. McGlynn*

Contribution from The Coates Chemical Laboratories, The Louisiana State University, Baton Rouge, Louisiana 70803, and the Department of Chemistry, Cumberland College, Williamsburg, Kentucky 40769. *Received August 29, 1974*

Abstract: Photoelectron spectra are reported for parabanic acid, three of its *N*-alkyl derivatives, and three *N*-alkyl derivatives of oxamide. The spectrum of parabanic acid is assigned using a composite molecule model based on a fragmentation into urea and/or *cis*-oxamide. The effects of *N*-methylation are discussed and used to differentiate various types of ionization events.

Previous papers in this series have been concerned with photoelectron spectra of various carbonyl-containing molecules and their interpretation in terms of composite models.[1,2] The present work represents an attempt to carry the composite molecule approach to a higher degree of complexity; it essays an interpretation of the PES of parabanic acid (imidazolidinetrione). Parabanic acid may be viewed

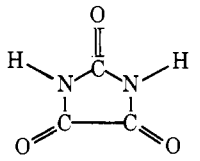

as a composite of: (i) urea and *cis*-glyoxal; (ii) a single carbonyl group and *cis*-oxamide; (iii) three carbonyl groups and two sp^2 hybridized nitrogens; (iv) two formamides and one carbonyl group; and (v) one imide and one amide. It will be shown that the composite molecule approach remains valid and that the partitioning of most utility is (i).

The effect of *N*-methylation on the ultraviolet absorption spectra of amides[3] and oxamides[4] has been a useful diagnostic tool in making distinction between $^1\Gamma_{\pi\pi^*} \leftarrow {}^1\Gamma_1$ and $^1\Gamma_{n\pi^*} \leftarrow {}^1\Gamma_1$ transitions. It is expected that similar diagnostic utility should reside in *N*-methylation effects on PES ionization energies. Thus, an n-MO largely localized on the >C=O groups should be much less sensitive to *N*-methylation than a π_O-MO which has large amplitude on the amine nitrogens. Indeed, it has been asserted[5] that such differential effects of *N*-methylation are responsible for a reversal of the two lowest energy PES bands of formamide, where $I(n) < I(\pi_O)$, on going to *N*-methylformamide, where $I(\pi_O) < I_{(n)}$. It is a purpose of the present work to investigate the diagnostic utility of *N*-methylation (or *N*-alkylation) in corroborating prior assignments[6] of the PES of oxamide and in making assignments of the PES of parabanic acid.

The MO notation used in the discussion of oxamides has been elaborated previously[1,6] and consists of the set $\{n_+, n_-, \pi_\oplus, \pi_\ominus, \pi_+, \pi_-\}$, the σ-MO's remaining undifferentiated. The MO notation used in the discussion[6] of urea consists of the set $\{n, \pi_\oplus, \pi_\ominus, \pi\}$. The MO notation which has been found useful in discussing parabanic acid consists of two subsets: $\{n_+, n_-, \pi_\oplus, \pi_\ominus, \pi_+, \pi_-\}$ of oxamide and $\{n, \pi\}$ of urea. It should not be supposed that these two subsets do not overlap; it may be inferred, however, that the overlap is small.

Experimental and Computational

Instrumentation and techniques have been described previously.[6] All chemicals were prepared and purified in these laboratories and are described elsewhere.[4,7]

Semiempirical CNDO/s-CI calculations[8] were carried out for *cis*-glyoxal, urea, parabanic acid, *N*-methylparabanic acid, and *N,N'*-dimethylparabanic acid at geometries appropriate to their ground states.[9]

Solid samples were sublimed directly in a heated probe, the temperature of which was adjusted for maximum count rate. The range of temperatures used was 72 to 119°; the temperature was always maintained at least 50° below the melting point of the solid. A continuous flow of vapor, at pressures always less than 40 μ, was maintained through the target area. No decomposition of any molecule studied in this work was noted under the conditions cited.

Results

The experimental PES data consist of ionization band energies, band intensities, vibronic structure associated with a given band, and *N*-methylation effects on band energies. The number of specific identifications of band type which can be made on the basis of such data is not very large. Nonetheless, in the discussion of this section we will append identifications to the majority of the observed bands. The justification for such identifications resides in correlative schemes based on CNDO/s computational results which will be discussed later and in the consistency of application of additivity rules which have been discussed previously.[1]

The photoelectron spectra of the oxamides are shown in Figure 1 and those of the parabanic acids are shown in Figure 2. The experimental PES data, with assignments, are shown in Table I.

The n_- band of these systems is the only one which consistently exhibits vibronic structure. The vibronic analyses of the n_- bands are detailed in Table II. The coupled vibration, in all instances, is the simple carbonyl stretching mode. The n_+ band is vibronically resolvable only in oxamide[6] where it exhibits skeletal modes as well as a carbonyl stretching mode. The 440 cm^{-1} mode which is coupled to this ionization event probably corresponds to the υ_8 (OCN bending mode, a_g) which, in the neutral molecule, occurs at 536 cm^{-1}. Consequently, we take the presence of low-frequency modes in the n_+ band of oxamide as a vindication of the "through-bond" coupling[10] of the n_+-MO and the σ-bonding MO framework of oxamide. The multiple vibronic coupling evident in the n_+ band of oxamide, as well as the indistinct resolution found in oxamide, provides a good rationale for our inability to resolve any vibrational structure in this band in any of the more complex molecules.

The lowest energy PES band of the alkyl oxamides is highly intense and, on the basis of relative cross sections, must be supposed to contain three distinct ionization events. This conclusion also follows from direct comparison with the oxamide spectrum: *N*-alkylation moves the $\pi_\ominus$ and $\pi_\oplus$

Table I. Ionization Energies and Band Assignments of Oxamides and Parabanic Acids[a] Band Energies (in eV)/Assignment

MOLECULE	I(1)	I(2)	I(3)	I(4)	I(5)	I(6)	I(7)	I(8)	I(9)	I(10)	I(11)	I(12)	I(13)
OXAMIDE	9.80(V)	10.50	11.04	11.72(V)	13.39(V)	14.50(V)	14.90	15.70	16.15	17.80	18.70		
OX	n_+	$\pi_\ominus$	$\pi_\oplus$	n_-	π_-	σ	σ	σ	π_+	σ	σ		
N,N'-DIMETHYLOXAMIDE	9.33	9.62	10.07	11.20(V)	12.42	13.66	14.26	15.33	16.5	18.35			
DMOX	n_+	$\pi_\ominus$	$\pi_\oplus$	n_-	π_-								
N,N,N',N'-TETRAMETHYL-OXAMIDE	9.02	9.08	9.34	10.49	12.0	13.90	14.46	15.12	16.20	17.9			
TMOX	n_-	$\pi_\ominus$	$\pi_\oplus$	n_-	π_-								
N,N'-DIPROPYLOXAMIDE	9.12	9.25	9.79	11.17(V)	11.84	12.70	13.79	14.89					
DPOX	n_-	$\pi_\ominus$	$\pi_\oplus$	n_-	π_-								
PARABANIC ACID	10.67	11.34	11.57	11.79	12.58[b]	14.10	14.57	15.55	15.75	16.3	16.8	17.55	18.8
PBA	n_+	$\pi_\oplus$	n	$\pi_\oplus$	n_-	π_-							
N-METHYLPARABANIC ACID	10.52	10.68	11.2	11.39	12.29[b]	13.73	14.43	15.60	16.10	16.7	17.6	18.1	19.6
MPBA	n_+	$\pi_\oplus$	n	$\pi_\ominus$	n_-	π_-							
N,N'-DIMETHYLPARABANIC ACID	10.19	10.33	10.97	11.1	12.19[b]	13.3(V)	14.19	14.87	15.24				
DMPBA	$\pi_\oplus$	n_+	$\pi_\ominus$	n	n_-	π_-	π_+						
N,N'-DIPROPYLPARABANIC ACID	9.90	10.10	10.65	11.90	12.15	12.63	13.90	15.15	16.3	17.0	19.0		
DPPBA	$\pi_\oplus$	n_+	$\{\pi_\ominus, n\}$	n_-									

[a] Vertical ionization energies are denoted by V; bands so denoted exhibit vibrational structure. [b] The vertical and adiabatic ionization energies are identical for these bands.

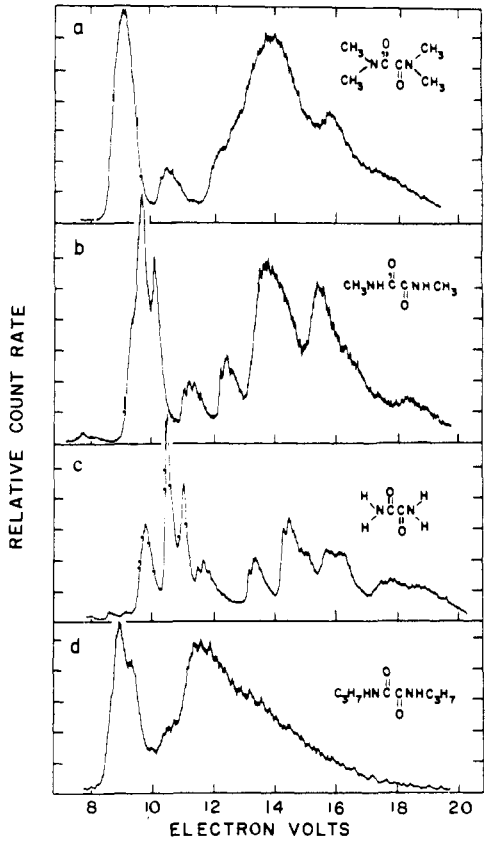

Figure 1. Photoelectron spectra of (a) *N,N,N',N'*-tetramethyloxamide (TMOX), (b) *N,N'*-dimethyloxamide (DMOX), (c) oxamide (OX), *N,N'*-di-*n*-propyloxamide (DPOX).

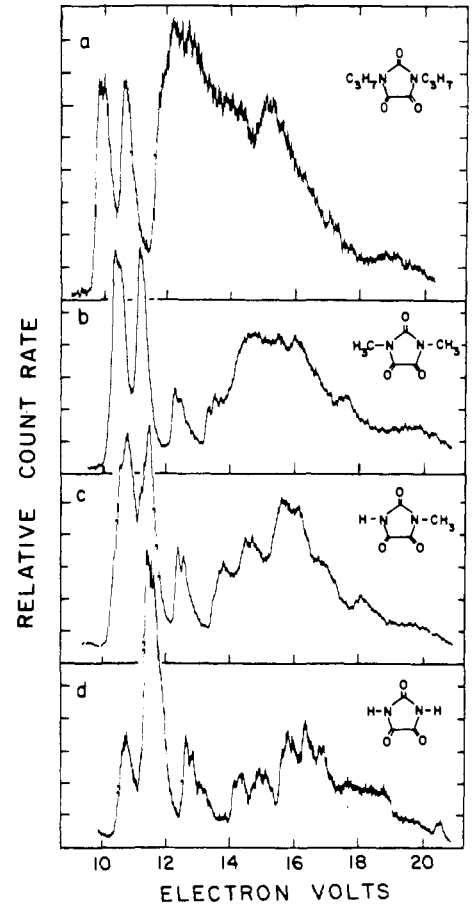

Figure 2. Photoelectron spectra of (a) dipropylparabanic acid (DPPBA), (b) dimethylparabanic acid (DMPBA), (c) methylparabanic acid (MPBA), and (d) parabanic acid (PBA).

bands toward lower ionization energies faster than it does the n_+ band; as a result, all three bands tend toward coincidence, and almost achieve coincidence in TMOX.

The 14 eV region of oxamide undergoes massive increase as a result of *N*-methylation. This region represents the location of new π and σ ionization events introduced by *N*-methylation. A similar statement applies to the 11-14 eV region of DPPBA.

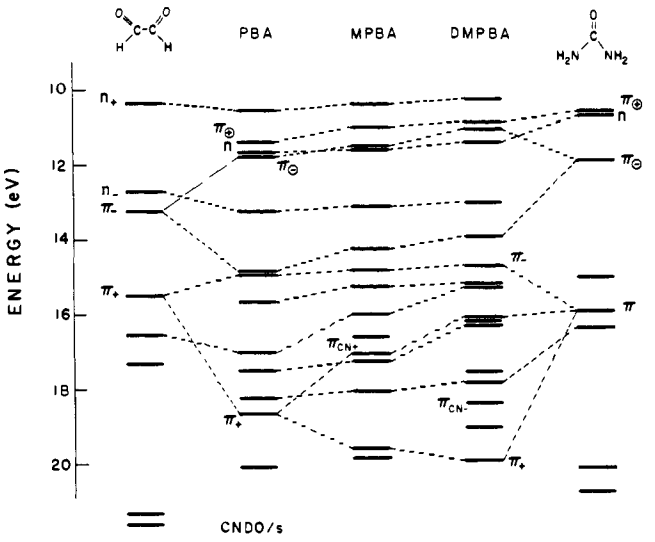

Figure 3. Computational CNDO/s correlation diagram for *cis*-glyoxal, PBA, MPBA, DMPBA, and urea molecules. The comparison of the two correlation diagrams of Figures 3 and 4, as also, the textual language, implies the use of Koopmans' theorem.[11] The computations of Figure 3 are for *cis*-glyoxal; the experimental PES data of Figure 4 are for *trans*-glyoxal.[13]

Table II. Vibronic Characteristics of the n_ Band

Molecule	No. of Vibronic peaks	ν_{Av}, cm^{-1}	ν in $^1\Gamma_1$, cm^{-1}	v^a
OX	6	1560	1700[b]	1
DMOX	5	1530	1650[c]	1
TMOX	5	1540	1660[d]	1
DPOX	Band occluded			
PBA	4	1550	1760[e]	0
MPBA	4	1700		0
DMPBA	4	1620		0
DPPBA	Band partially occluded			

[a] The number of quanta of the carbonyl stretching mode which, superposed in I(adiabatic), yields I(vertical). [b] J. R. Durig, S. C. Brown, and S. E. Hannum, *Mol. Cryst. Liq. Cryst.*, 14, 129 (1971). Assuming maintenance of symmetry in the ionic state, the observation of a progression in the 1560 cm^{-1} interval is adequate to identify this interval as the $\nu_3(a_g)$ mode of OX^+ and to eliminate the $\nu_{19}(b_u)$ possibility. [c] T. Miyazawa, T. Shimanouchi, and S. Mizushima, *J. Chem. Phys.*, **24**, 408 (1956). [d] D. B. Larson, Ph.D. Dissertation, Louisiana State University, Baton Rouge, Louisiana, August 1972. [e] A. Alemagna and V. Lorenzelli, *J. Chim. Phys. Phys.-Chim. Biol.*, 61, 884 (1964).

The intense, 11-12 eV, band of PBA contains three ionization events: $\pi_\oplus$, n, and $\pi_\ominus$, which correspond to the 11.34, 11.57, and 11.79 eV PES features. However, the precise order of correspondence is not known. The energy of the n_ band is quite insensitive to *N*-alkylation, as is also the n_+ band. The effects of *N*-alkylation are to move the $\pi_\oplus$ and $\pi_\ominus$ bands toward the n_+ band in such a way that, in DPPBA, the lowest energy ionization event is $\pi_\oplus$. The energy of the $\pi_\oplus$ band is somewhat more sensitive than that of $\pi_\ominus$, with the result that these bands become more distinct as a result of methylation. The effects of methylation on the n ionization are somewhat more difficult to follow; however, it does appear that the n and $\pi_\ominus$ events also invert on proceeding from PBA to DMPBA.

The 14.73 eV band of PBA remains distinct in all four compounds and encroaches, as a result of increasing *N*-alkylation, on the n_ band. This 14.73 eV band of PBA is identified, as a result, as the π_- band. This band lies at

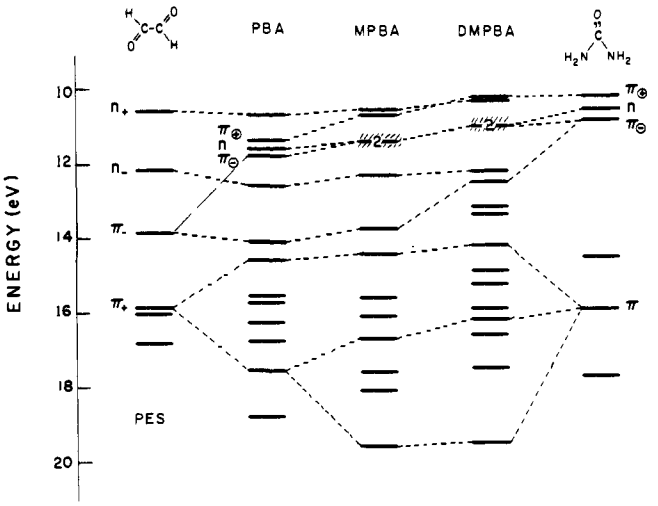

Figure 4. Experimental PES correlation diagram for *trans*-glyoxal,[13] PBA, MPBA, DMPBA, and urea molecules.

13.11 eV in DMPBA and exhibits a weakly defined vibrational progression in an 800 cm^{-1} interval.

Discussion

A consideration of ionization potentials devolves, via Koopmans' theorem,[11] to a consideration of molecular orbitals. Hence, a brief resumé of the types of orbitals which CNDO/s calculations provide for parabanic acids is given and these orbitals are related to those of the two entities, *cis*-oxamide and urea, into which parabanic acid is most aptly partitioned.

The effects of *N*-methylation are discussed from both computational and experimental points of view, and the two views are shown to be concordant. The viability of *N*-methylation as a diagnostic tool is validated.

Finally, CNDO/s results are correlated with the experimental ionization data and the assignments given in Table I are, to some extent, validated.

Molecular Orbitals of Parabanic Acids. The highest energy filled MO of the parabanic acids, DMPBA and DPPBA being possible exceptions, is of σ type, is largely localized on the oxygens of the α-dicarbonyl group, but also possesses considerable σ-bonding character of carbonyl-carbonyl nature, and, following Swenson[10] and Cowan et al.,[12] is classified as n_+. All other n orbitals lack the intercarbonyl bonding characteristic. The n-MO is essentially identical with that of urea, and is almost entirely situated on the oxygen of the isolated carbonyl group. The n_-MO is the most delocalized of all n-MO's, possesses amplitude on all three oxygen centers, but retains a dominant *cis*-glyoxal identity.

The $\pi_\oplus$-MO's are heavily localized on the amine residues and are essentially nonbonding. The highest energy π_O-MO is $\pi_\oplus$; the $\pi_\oplus$-MO embraces both the N centers and all three carbonyl centers, and is N (C=O) antibonding in all instances. The $\pi_\ominus$-MO is similarly antibonding but possesses a node at the isolated carbonyl group. The $\pi_\oplus$-MO's are very similar to the corresponding $\pi_\oplus$ pair of urea but also possess one-to-one correspondences with the $\pi_\oplus$ pair of *cis*-oxamide. The $\pi_\oplus$-MO's possess large amplitudes on the nitrogen centers, ~50%; consequently, they are expected to be very sensitive to *N*-methylation. In contrast, N amplitudes for the {n_+, n_, n}-MO set are usually less than 8%, hence, their insensitivity to *N*-methylation.

The π_--MO is entirely *cis*-oxamide localized and is highly N-C-O π bonding. It contains ~40% amplitude on the N centers and this, coupled with its highly conjugative

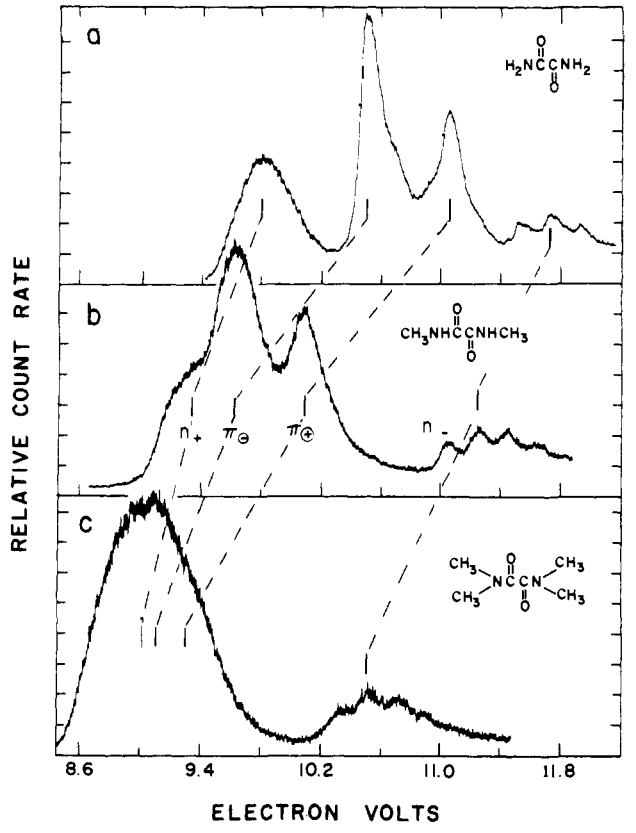

Figure 5. High-resolution photoelectron spectra of the low-energy ionization region of (a) OX, (b) DMOX, and (c) TMOX.

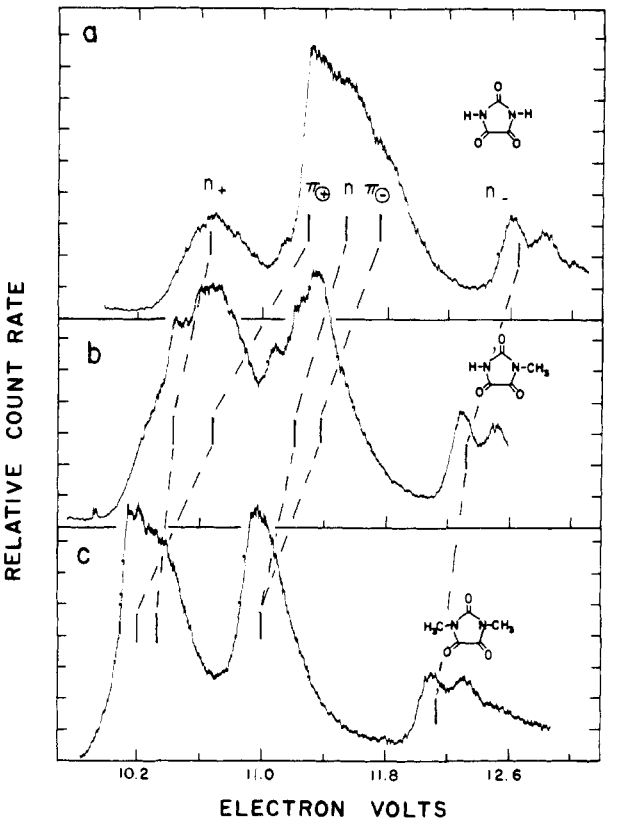

Figure 6. High-resolution photoelectron spectra of the 10-13 eV region of (a) PBA, (b) MPBA, and (c) DMPBA.

Table III. *N*-Alkylation Shifts (eV) in the PES of Oxamides

Molecule		$I(n_+)$	$I(\pi_\ominus)$	$I(\pi_\oplus)$	$I(n_-)$	$I(\pi_-)$
OXAMIDE		0.0				
DMOX	Exptl	−0.47	−0.88	−0.97	−0.52	−0.97
	Calcd	−0.25	−0.62	−0.51	−0.28	−1.22
TMOX	Exptl	−0.78	−1.42	−1.70	−1.23	−1.39
DPOX	Exptl	−0.68	−1.25	−1.25	−0.55	−1.55(?)

Table IV. *N*-Alkylation Shifts (eV) in the PES of Parabanic Acids

Molecule		$I(n_+)$	$I(\pi_\oplus)$	$I(n)$	$I(\pi_\ominus)$	$I(n_-)$	$I(\pi_-)$
PBA	Exptl	0.0					
	Calcd	0.0					
MPBA	Exptl	−0.15	−0.66	−0.37	−0.40	−0.29	−0.37
	Calcd	−0.16	−0.39	−0.13	−0.23	−0.14	−0.59
DMPBA	Exptl	−0.48	−1.15	0.47	−0.82	−0.39	−0.80
	Calcd	−0.30	−0.33	−0.26	−0.70	−0.27	−0.93
DPPBA	Exptl	−0.57	−1.44	−0.92	−1.14	−0.68	

N-C-O nature, should make it exceedingly sensitive to *N*-methylation.

The π_+-MO of *cis*-glyoxal splits into two in parabanic acid. The one of higher energy has a node between the glyoxal and urea residues and is ~60% urea localized. This MO is termed π and is very similar to the corresponding MO of urea. The other component, which we term π_+, is ~80% localized on the *cis*-oxamide fragment, hence, our retention of the π_+ designation. The π-MO has less than 5% density on the N centers, whereas that of the π_+-MO is ~40%. As a result, the sensitivity of these MO's to *N*-methylation effects is expected to be quite variant.

The introduction of methyl groups introduces another subset of MO's, some of which are highly conjugative. The effects of this conjugation are most obvious in the π_+-MO, which happens to be quasi-degenerate with the pseudo-π-MO of the CH_3 group. The effects of π conjugation with the CH group(s) are shown, in self-evident notation, in Figures 3 and 4.

***N*-Alkylation.** The effects of *N*-methylation on the lower energy set of ionizations of oxamide are shown in Figure 5. All four ionizations move to lower energies; those designated as $I(n_+)$ and $I(n_-)$ are much less sensitive than $I(\pi_\oplus)$ and $I(\pi_\ominus)$. The effects of various *N*-alkylations on oxamide ionization energies are tabulated in Table III. It seems clear that this technique is a useful means of distinguishing between n and π ionization events.

The effects of *N*-alkylation on the ionization energies of parabanic acid (PBA) are illustrated in Figure 6 and are tabulated in Table IV, where they are compared with predictions based on CNDO/s computations. It seems clear, from both computational and experimental evidence, that the diagnostic value of *N*-methylation in n/π discrimination is considerable.

It will be noted that the two π_O bands diverge, as a result of *N*-alkylation, in the parabanic acids, whereas they converge in the oxamides. It will also be noted that the $\pi_\ominus/\pi_\oplus$ order is inverted in these two sets of molecules. This inversion, as a computational result, is vested in the cis/trans "isomerism" which may be supposed to differentiate between the two sets of compounds. This cis/trans "isomerism", the resultant $\pi_\ominus/\pi_\oplus$ inversion, and consistently greater sensitivity of the $\pi_\oplus$-MO to *N*-methylation effects produces the divergency/convergency characteristics which typify the photoelectron spectroscopic effects found in the oxamide/parabanic acid molecules.

It is appropriate to emphasize that the least resolved spectrum is that of TMOX (see Figure 5). It is probable that much of this diffuseness is associable with a possible

sterically induced nonplanarity of TMOX. Unfortunately, the only information available on this point relates to NMR studies, and inferences based thereon by Siddall and Good.[14] In any event, such a nonplanarity would lead to an expected decrease in the $\pi_\ominus/\pi_\oplus$ separation, the n_+/n_- separation remaining relatively unaffected. Consequently, it is possible that the near degeneracy of the n_+, $\pi_\oplus$, and $\pi_\ominus$ ionization events exhibited in Figure 5c is attributable, in part, to bending and not *solely* to *N*-methylation effects as implied above. In addition, the diffuseness of the 9 eV PES band may be due not so much to near degeneracy of these three events (i.e., the n_+, $\pi_\oplus$, and $\pi_\ominus$ ionizations) as to the existence of a statistical ensemble of variously twisted TMOX species in the gas phase.

Correlation Diagrams. The results of CNDO/s computations are summarized in Figure 3 and may be compared with the experimental correlation diagram of Figure 4. This comparison is massively impressive, particularly in the lower ionization energy regime. Any assignments which might be made in the higher ionization energy regime (apart from direct comparison with the computational results, a procedure which is more than suspect) would have little foundation; hence, this region is left largely unassigned.

Acknowledgment. This work was supported by contract between the United States Atomic Energy Commission-Biomedical and Environmental Research Physics Program and The Louisiana State University.

References and Notes

(1) J. L. Meeks, H. J. Maria, P. Brint, and S. P. McGlynn, *Chem. Rev.*, in press.
(2) J. L. Meeks, J. F. Arnett, D. B. Larson, and S. P. McGlynn, *Chem. Phys. Lett.*, **30**, 190 (1975).
(3) H. Basch, M. B. Robin, and N. A. Kuebler, *J. Chem. Phys.*, **49**, 5007 (1968).
(4) D. B. Larson and S. P. McGlynn, *J. Mol. Spectrosc.*, **47**, 469 (1973).
(5) C. R. Brundle, D. W. Turner, M. B. Robin, and H. Basch, *Chem. Phys. Lett.*, **3**, 292 (1969).
(6) J. L. Meeks, J. F. Arnett, D. B. Larson, and S. P. McGlynn, *J. Am. Chem. Soc.*, **97**, 3905 (1975).
(7) D. B. Larson, J. F. Arnett, and S. P. McGlynn, *J. Am. Chem. Soc.*, **95**, 6928 (1973).
(8) The program used was QCPE:CNDO 174.
(9) Geometrical parameters used in CNDO/s were: bond lengths and bond angles for PBA were those of D. R. Davis and J. J. Blum, *Acta Crystallogr.*, **8**, 129 (1955). Standard structural parameters were used for the CH_3 groups of PBA derivatives. Urea: A. Caron and J. Donahue, *ibid.*, **17**, 544 (1964). *cis*-Glyoxal: E. M. Ayerst and J. R. C. Duke, *ibid.*, **7**, 588 (1954).
(10) J. R. Swenson and R. Hoffmann, *Helv. Chim. Acta*, **53**, 2331 (1970).
(11) T. Koopmans, *Physica* (Utrecht), **1**, 104 (1934).
(12) D. O. Cowan, R. Gleiter, J. A. Hashmall, E. Heilbronner, and V. Hornung, *Angew. Chem., Int. Ed. Engl.*, **10**, 401 (1971).
(13) D. W. Turner, C. Baker, A. D. Baker, and C. R. Brundle, "Molecular Photoelectron Spectroscopy", Wiley-Interscience, New York, N.Y., 1970.
(14) T. H. Siddall and M. L. Good, *J. Inorg. Nucl. Chem.*, **29**, 149 (1967); M. L. Good, T. H. Siddall, and R. N. Wilhite, *Spectrochim. Acta, Part A*, **23**, 1161 (1967).

Nicotinamide Adenine Dinucleotide (NAD^+) and Related Compounds. Electrochemical Redox Pattern and Allied Chemical Behavior

Conrad O. Schmakel, K. S. V. Santhanam, and Philip J. Elving*[1]

Contribution from The University of Michigan, Ann Arbor, Michigan 48104.
Received November 26, 1974

Abstract: Important aspects of the electrochemical redox pattern and related chemical behavior of nicotinamide adenine dinucleotide (NAD^+) have been examined on the basis of electrochemical, spectrophotometric, chemical, and enzymatic studies of the coenzyme, $NADP^+$, deamino-NAD^+, their reduction products, and related nicotinamides and adenines. The artifacts introduced into the observed electrochemical patterns by coenzyme and reduction product adsorption at the solution–electrode interface can be removed by addition of a more strongly adsorbed species. An initial reversible one-electron (1e) addition to the pyridinium ring produces a free radical, which dimerizes (rate constants at pH 9 and 30° are $2.4 \times 10^6\ M^{-1}$ sec^{-1} for NAD^+, 1.6×10^6 for $NADP^+$ and 1.7×10^6 for deamino-NAD^+; activation energies and frequency factors were determined). At more negative potential, the radical is reduced (1e, 1 H^+) to a dihydropyridine, largely 1,4-NADH; some 1,6-NADH is also formed, indicating the lesser specificity of electrochemical reduction as compared with enzymatic. At sufficiently positive potential, dimer and dihydropyridine are oxidized to NAD^+; the dimer is much more easily oxidized. The dimer is not directly reduced electrochemically within the available potential range. Both reduction products hydrolyze; rate increases with decreasing pH; at a given pH, dimer is less stable than dihydropyridine.

The pyridine nucleotide, nicotinamide adenine dinucleotide (NAD^+; diphosphopyridine nucleotide, DPN^+; coenzyme I) (Figure 1), is a coenzyme for the dehydrogenase enzymes which catalyze redox processes in virtually all biological systems, involving transfer of hydrogen between substrate and coenzyme, e.g., alcohol dehydrogenase (ADH) catalyzes oxidation of ethanol to acetaldehyde and simultaneous reduction of NAD^+ to $NADH^2$ via effective net transfer of a hydride ion from alcohol to C(4) of the pyridine ring.[3]

The gross reversibility of the NAD^+/NADH redox couple under physiological conditions has prompted extensive study by polarographic techniques.[4] While the basic reduction pathway of NAD^+ has been well established (cf. Redox Path), certain aspects of its electrochemical and related chemical behavior have been only partially explained or have not been considered. The present investigation was designed to establish more clearly the influence of adsorption of reactant and products at the interface, the postulated electroactivity of the dimer produced on the initial one-electron (1e) reduction, the structure of the product(s) produced on 2e reduction, the magnitudes of rate-controlled